ELSEVIER

Monitoring state-of-charge of Ni–MH and Ni–Cd batteries using impedance spectroscopy

Abderrezak Hammouche*, Eckhard Karden, Rik W. De Doncker

Institute for Power Electronics and Electrical Drives, Aachen University of Technology, Jägerstrasse 17–19, D-52066 Aachen, Germany

Abstract

This paper reports on laboratory studies into the ac impedance spectra of nickel–metal hydride and nickel–cadmium batteries, aiming at finding out possible correlation between electrical parameters, extracted directly from the high frequency region, and the battery state-of-charge (SoC). Impedance diagrams were recorded immediately after interrupting the dc charge, or discharge, current. The study revealed that the series resonance frequency, at which the dynamic cell behavior switches from an inductive character ($Z'' > 0$) to a capacitive one ($Z'' < 0$), varied monotonously as a function of state-of-charge. This behavior was reproducible after intermittent charge and discharge. Half-cell measurements were also conducted to associate the cell impedance with either processes occurring at the positive or negative plates.
© 2003 Elsevier B.V. All rights reserved.

Keywords: Ni–MH; Ni–Cd; Battery state-of-charge; Impedance spectroscopy; Series resonance frequency

1. Introduction

Sealed nickel–metal hydride and nickel–cadmium secondary batteries, have demonstrated a rapid expansion in many areas of battery usage. For practical purposes, a technique capable of predicting the residual capacity with sufficient accuracy is urgently required. This applies particularly to the new 42 V-system where the battery is strained to a state-of-charge (SoC) as low as 40%. Traditional solutions used for vented lead–acid cells, such as specific gravity or electrolyte resistance measurements, cannot be applied to these sealed systems because the cell electrolyte composition remains virtually constant during charge–discharge cycles. The only reliable procedure to determine battery SoC and aging effects is to perform a complete discharge–charge cycle. This operation is obviously expensive, time-consuming and leaves the batteries to be tested out of service during the testing time.

Impedance spectroscopy is used to make a fast, non-destructive and reliable method for such a characterization. The objective consists of inferring from the impedance spectra, plotted in different conditions, one or many electrical parameters, which increase or decrease monotonically as a function of the battery SoC. Such parameters should

be: (i) simple to measure; (ii) reproducible; and (iii) quickly accessible.

Research in laboratories on impedance parameters related to state-of-charge or state-of-health of battery cells has been carried out over the last two decades [1–4]. Hampson et al. [5], Huet [6] and Rodrigues et al. [7] reviewed the published data on impedance studies of batteries and battery electrodes, undertaken for this purpose. It has been shown that various parameters may be useful to estimate the status of battery systems under different experimental conditions (under load or at open circuit after a period of rest), particularly of lead–acid and nickel–cadmium secondary batteries, but little thorough work on impedance parameters related to Ni–MH batteries has been done so far [8].

Earlier measurements conducted on alkaline batteries [2,3,9,10], investigating cell response in the high frequency domain, were not conclusive because the electrolyte does not participate to the overall electrode processes, whereas a pronounced effect of SoC was observed on those electrical quantities extracted from the low frequency region of the impedance diagrams, such as the impedance modulus, the phase angle, the equivalent series and parallel capacitance of the cell. However, it should be noted that measurements at low frequencies are time-consuming and, hence, less suitable for routine monitoring of cells in service.

Besides, most of these studies were concerned with small capacity batteries, typically less than 10 Ah. Such cells generally present impedance magnitudes ranging from some

* Corresponding author. Tel.: +49-241-80-96973;
fax: +49-241-80-92203.
E-mail address: hm@isea.rwth-aachen.de (A. Hammouche).

tens of milliohm up to several ohms, depending on the measuring frequency and SoC. Several commercial impedance meters exist in the market which enable experimental measurement of such impedances. However, for larger capacity batteries, the impedance magnitude falls well below the milliohm range. As a result, more precise and reliable instrumentation is needed [11].

The aim of the present study is to scrutinize the high frequency region of the cell impedance spectra in order to evince possible relationship between high frequency electrical parameters and SoC. The investigation was undertaken on two kinds of rechargeable alkaline batteries: Ni–MH and Ni–Cd systems with relatively large capacity, using dedicated high-precision instrumentation.

2. Experimental

Measurements were carried out on vented Ni–Cd batteries manufactured by Hoppecke under the reference name FNC-T 204H, with a nominal capacity of 46 Ah cells. The cells were first conditioned at room temperature for a few cycles, using a Digatron test facility, to stabilize their discharge capacity. They were cycled by charging first at $C/2$ rate to reach 60% SoC and further at $C/10$ rate to achieve a total overcharge factor of 1.4. After a rest for 5 min, the cells were discharged at $C/5$ rate to a cut-off voltage of 1.0 V.

Sealed prismatic Ni–MH cells with a rated capacity of 42 Ah (Varta NP 42) were also studied. They were cycled, as specified by the manufacturer, by charging at C rate to reach 80% C, resting for 5 min and followed by further charging 30% of the nominal capacity at $C/5$ rate. The discharge operation was made with a C rate to a cut-off voltage of 1.0 V.

Impedance measurements were conducted at various states of charge, stepped with approximately 10% SoC, on open circuit, immediately after charge or after discharge. Starting at the fully discharged state, the cells were charged intermittently at $C/5$ rate for $1/2$ h to achieve increasing SoCs. They were systematically discharged at $C/5$ down to 1.0 V after plotting the impedance spectra, to determine their actual state-of-charge, before recharging to the next SoC. Impedance spectra were also recorded at different SoCs immediately after intermittent discharges.

Laboratory instrumentation, used for the present experiments, has been developed at ISEA for high-precision impedance measurements on industrial batteries [12]. In order to ensure that impedance measurements are performed under linear conditions, the ac current amplitude was automatically chosen for each frequency so that the maximum ac voltage response was equal to 3 mV. In such conditions, the variation in SoC induced by the ac signal during impedance measurements, does not exceed 0.03% for the lowest frequency used. The frequency domain investigated ranged from 3 kHz down to 0.1 Hz, occasionally to 0.01 Hz, with a frequency distribution of 24 frequencies/decade.

Great care has been taken for measuring the low impedances of the cells. The significant contribution of the connecting leads to the measured impedance has been eliminated by using four leads; two for the current flow and the other two for the voltage measurement.

For half-cell measurements, to separately estimate each electrode polarization and impedance for the vented Ni–Cd cell, a mercury/mercurous oxide reference electrode (RE), of standard design, in the same potassium hydroxide concentration as the cell electrolyte, was employed. The RE tip was located in the midpoint of the free liquid electrolyte above the plates, between the two current collecting tabs. In the case of sealed Ni–MH batteries, certain impedance measurements have been performed using the cell case as a reference electrode, as was suggested by Reid [13] for impedance studies of sealed Ni–Cd cells. The voltage of the case with respect to the anode or cathode is unimportant provided that it remains stable during the measurement of the impedance. We checked systematically that the sum of the electrodes potential and impedance match exactly the corresponding cell quantities.

All ac impedance spectra reported in this paper were obtained at laboratory room temperature of $25 \pm 1\,^\circ$C.

3. Results and discussion

In previous studies, the cell impedance was measured in two distinct conditions: either during current flow [2,8,14], or at zero dc current after many hours of rest at open circuit [3,4,8]. The experimental data were then analyzed in light of models to derive useful fitting parameters. In the former case, the system is not in the steady-state conditions (i.e., the state-of-charge continuously drifts, especially during low frequency measurement), which complicates system modeling. The latter case could, however, be reasonably applied only to applications where time is not critical.

In the present experiments, we propose, for practical purposes, to exploit the raw data recorded immediately after interrupting the dc charge or discharge current. Furthermore, data obtained from the high frequency domain is used to derive electrical quantities at specific frequencies or from a narrow frequency interval.

3.1. Nickel–cadmium batteries

Fig. 1 shows the Nyquist loci for Ni–Cd cell at different SoCs, plotted after intermittent charge steps. The shape of the diagrams is basically the same, allowing to perform a unique exploitation of the data. At high frequencies, it displays a pronounced inductive effect. A semi-circle with a depressed shape appears at mid-frequencies, and prolonged by a low frequency tail. The intercept of the spectra with the real axis is labeled R_Ω. This term corresponds to the sum of the ohmic resistances of the electrolyte in the separator, the
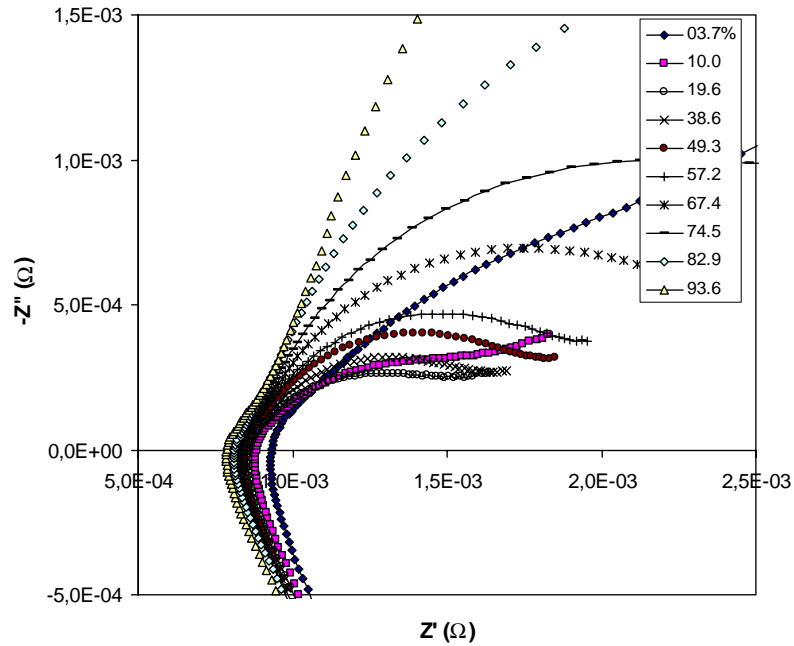
Fig. 1. Impedance spectra of 46 Ah Ni–Cd battery at different SoCs.

electrode active materials, the surface coverage of the electrodes by reaction products, and the connections inside the cell.

The size of the impedance diagram does not change monotonically with SoC: it decreases from a relatively large value at fully discharged state, passing through a minimum at 20% SoC and re-increasing for the higher SoC values.

In order to help determine which electrode is responsible for loss of cell performance, the impedances of positive and negative plates were plotted separately. Their algebraic sum systematically matches the cell impedance (Fig. 2), with the major contribution coming from the negative plates. Xiong et al. [15] arrived at the same conclusion using a galvanostatic non-destructive test method, which consists of recording the variations of the battery voltage, near the cell

equilibrium (within 2–3 mV) when applying a very small dc current.

From the general shape of these plots, it appears that the impedance imaginary part, Z'', changes more significantly, in the mid-frequency range, than the corresponding real part. Therefore, for a better resolution, it is more convenient to plot the variations of Z'' than the modulus. Fig. 3 shows the variations of Z'' at fixed frequencies (i.e., 10, 1 and 0.1 Hz). It can be noticed that after a decrease between 0 and 20% SoC, this parameter increases again at higher SoC, pronouncedly at 0.1 Hz.

As mentioned above, parameters that can be extracted from the high frequency domain of the impedance diagrams are preferable. In this respect, we examined the variations of the resistance R_Ω at which the impedance locus crosses the
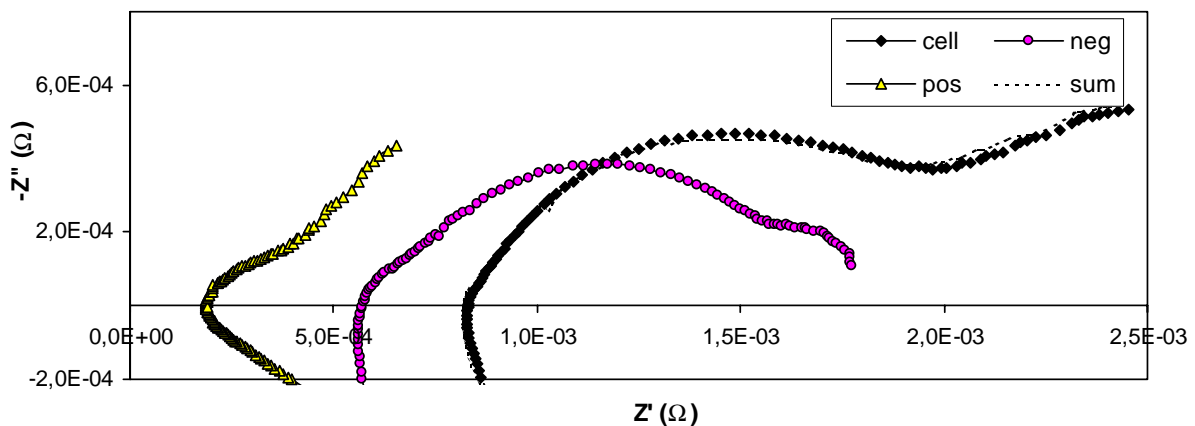

Fig. 2. Typical impedance diagrams of half-cells and complete Ni–Cd cell, at 57% SoC.
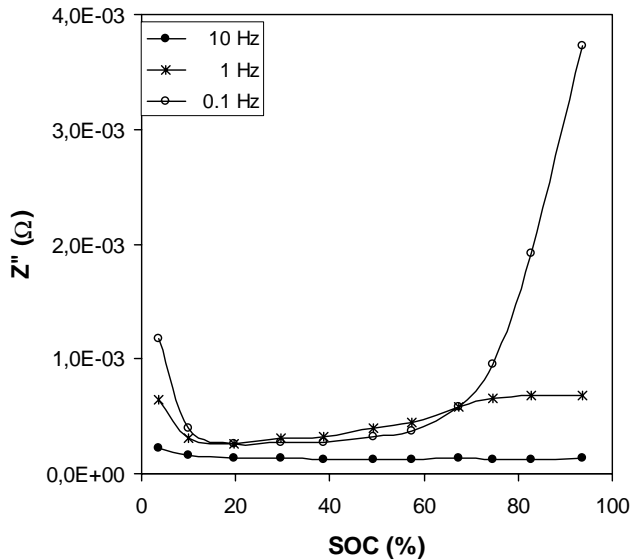
Fig. 3. Variations of the *iso*-frequency imaginary part measured at 10, 1 and 0.1 Hz for Ni–Cd battery.

real axis. Fig. 4 shows that this parameter is hardly usable to accurately estimate SoC due to its minor variations over the 20–100% SoC interval.

Unlike lead–acid batteries, in which the term R_Ω exhibits significant variations due to depletion of H_2SO_4 concentration during discharge, the contribution of the electrolyte in alkaline batteries is expected to be unimportant since KOH concentration remains globally constant during battery operation. This made all former investigations privilege the low frequency domain to deduce SoC indicating parameters. The slight increase observed in R_Ω, on discharge, is likely related with the presence of a substantial amount of poorly conducting $Ni(OH)_2$ at low SoCs [16]. This hypothesis is confirmed by observing an equivalent shift in the R_Ω term on the impedance of the positive plates; the negative plates show no evolution in this parameter.

A second high frequency parameter that can be exploited from the intercept of the spectra with the real axis
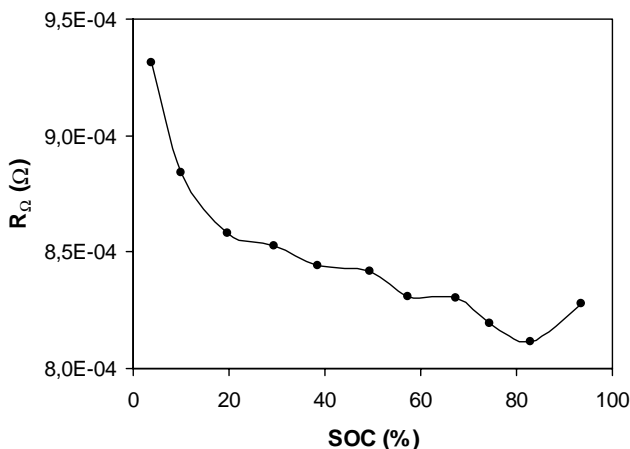

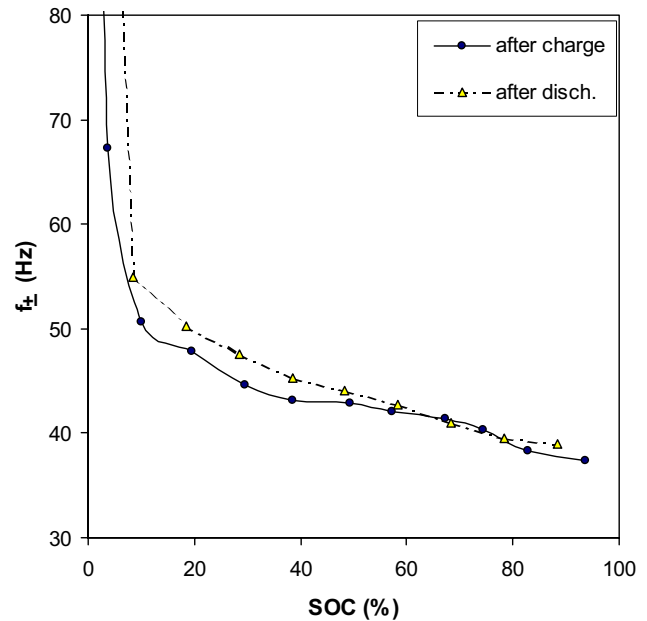Fig. 4. Evolution of the ohmic resistance with SoC for Ni–Cd battery.

Fig. 5. Series resonance frequency for Ni–Cd battery at different SoCs.

is the frequency at which the impedance passes through series resonance, $f_\pm$, being inductive ($Z'' > 0$) at higher frequencies and capacitive ($Z'' < 0$) at lower frequencies. Determining this parameter, denoted hereafter as $f_\pm$, needs interpolation of this part of the spectrum around the zero imaginary impedance. Fig. 5 shows that $f_\pm$ exhibits monotonous sensitivity to SoC, and so can be used as an indicator for the battery state-of-charge. Interestingly, the figure also shows that the same trend is obtained after intermittent discharges, giving much credibility to $f_\pm$ parameter in inferring battery SoC disregarding the battery operation history.

Unlike previous works, in which the inductive branch was systematically omitted, in the present work, we emphasize the 300–30 Hz frequency region where the inductive behavior is strongly present. In this region, the cell has mixed inductive–capacitive dynamic behavior extending on either side of this transition frequency. The resulting impedance diagram is consequently strongly deformed. This can be better viewed when Z'' is presented as a function of log(f) showing how steeply the curve intercepts the frequency axis. In the opposite case, where these two behaviors are unambiguously uncoupled, concentrated points are present in the vicinity of $f_\pm$ [17]. Such a mixed (inductive–capacitive) dynamic behavior is a specific feature of electrochemical power sources in view of their low-resistance and large-electrode capacitance. The inductive effect can be minimized by using the 4-contact measuring procedure and by twisting the electrical wires, but cannot be completely suppressed since the cell contains at least part of the leads. The value of the inductance for the present cells amounts to approximately 50 nH, deduced from 500 to 200 Hz interval in which the curve appears quite vertical. For reproducible measurements, the
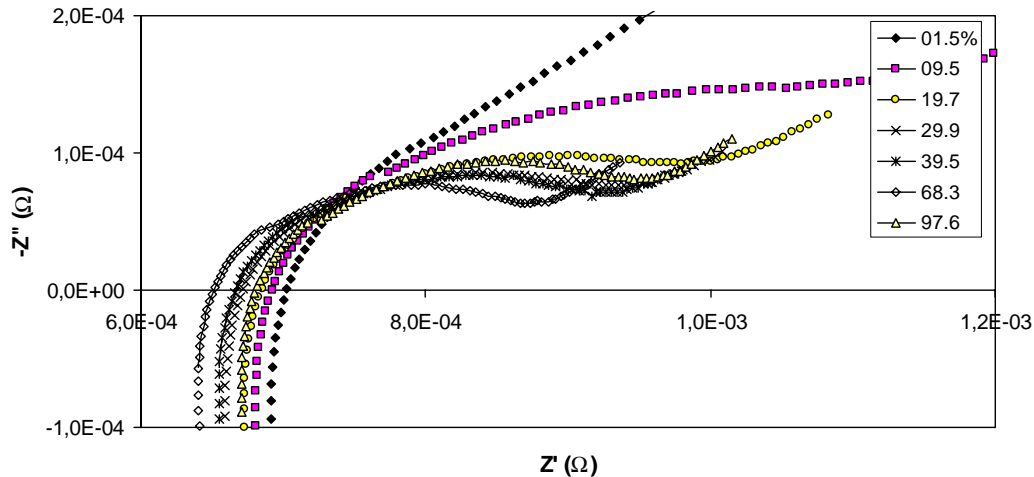
Fig. 6. Impedance spectra of 42 Ah Ni–MH battery at different SoCs.

connections must be built in a well-defined geometrical arrangement.

3.2. Nickel–metal hydride batteries

Fig. 6 shows the Nyquist plots for Ni–MH battery at some SoCs recorded immediately after switching off the dc charge current. The diagrams are composed of a semi-circle-like loop, which changes into a straight line as the frequency decreases. Apparently, while the shape does not change much with SoC, the whole impedance diagram shifts towards lower Z values when SoC increases in the 0–90% range. However, for 100% SoC, the opposite trend is observed, consistently with data on similar cells having a lower capacity [8].

On Fig. 7, the impedance of the positive and negative plates, measured against the cell case, is given. The sum of the half-cell impedance results fits the two-electrode measurement, confirming the validity of the measurement. Careful examination of the plates impedance shows that the variations observed in the cell impedance are induced basically by the evolution of the impedance of the positive plates, which shows variations with SoC parallel to those corresponding to the cell; the impedance of the negative plates does not vary with SoC. The positive electrode impedance is likely related to the presence of nickel hydroxide blocking films, reflected in the linear spike appearing in the low fre-

quency region for both of Ni–Cd and Ni–MH cells (Figs. 2 and 7). The behavior of the negative plates has been reported by Zhang et al. [18], who found the charge-transfer resistance of the MH electrode to be practically independent of its SoC, since this electrode does not undergo any significant structural modification during charge–discharge reactions, as these involve only absorption and desorption of hydrogen atoms in the alloy lattice.

Half-cell measurements show particularly that the re-increase of Z at 100% SoC comes from changes in the behavior of the positive plates during overcharge. Actually, the charge-transfer resistance associated with oxygen evolution during the overcharge process is higher than that corresponding to the main redox couple of the battery [19].

To detect a useful correlation between impedance parameters and battery SoC, we examined the evolution of some electrical parameters as for Ni–Cd batteries. From the general shape of these impedance plots, it can be noticed that the impedance real part, Z', changes more significantly, in the mid-frequency range, than the corresponding imaginary part. Fig. 8 shows that this quantity, measured at three fixed frequencies (i.e., 10, 1 and 0.1 Hz), displays a concave shape, going through a minimum extending between 50 and 95% SoC. Hence, the state-of-charge cannot be determined from the value of real component at a fixed frequency.

The ohmic resistance, R_Ω, decreases slowly upon charge, but re-increases for SoC greater than 80% (Fig. 9). This
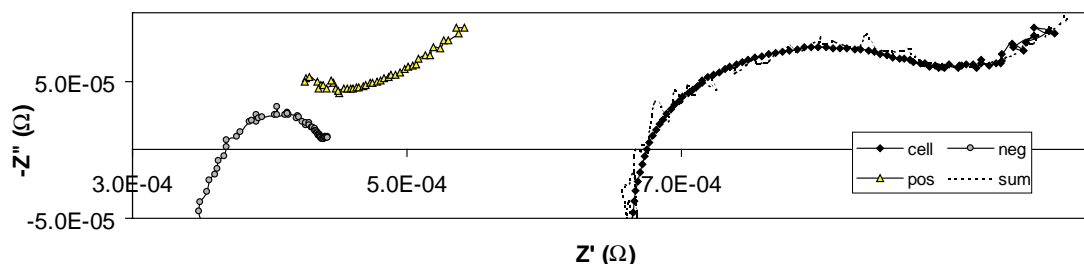

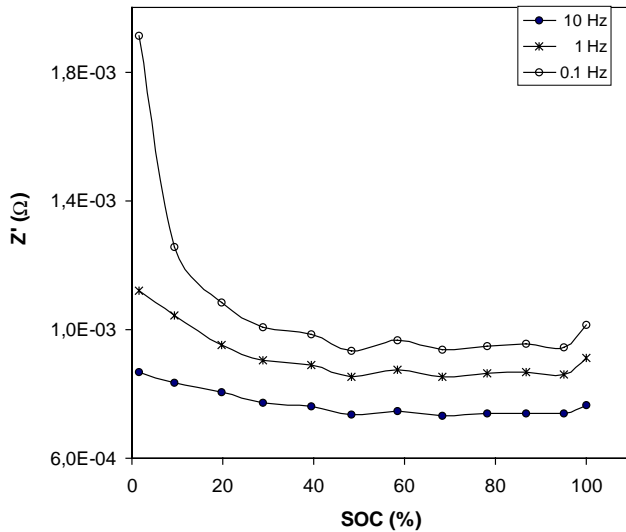Fig. 7. Typical impedance diagrams of half-cells and complete Ni–MH cell, at 30% SoC.

Fig. 8. Variations of the *iso*-frequency real part measured at 10, 1 and 0.1 Hz for Ni–MH battery.

Fig. 10. Series resonance frequency for Ni-H battery at different SoCs.

tendency is similar to what is reported above for Ni–Cd batteries. The positive reaction product, formed upon discharge, and gas dissolution in the electrolyte, produced in the overcharge conditions, are respectively, responsible for the increase of R_Ω at low and high SoC values. Moreover, the small differences measured do not allow accurate determination of SoC from this parameter.

Similar to Ni–Cd batteries, the only parameter that displays monotonous variations with SoC is the series relaxation frequency $f_\pm$ (Fig. 10). It increases continuously from about 95 Hz, for the 100% SoC, up to 150 Hz, for the fully discharged state. Of particular importance, is the reproducibility of $f_\pm$ values recorded upon battery discharge,
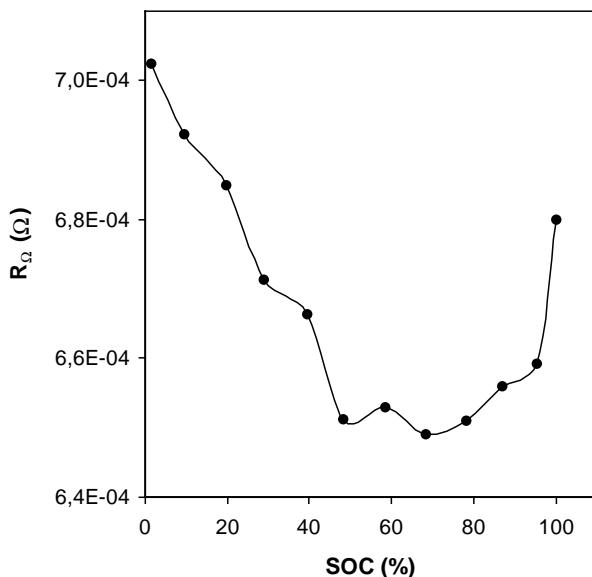
showing the robustness of such a parameter in inferring the battery SoC irrespective of whether the battery has just been charged, or discharged.

4. Conclusions

In this work, we looked for possible correlation between certain electrical parameters derived directly from experimental impedance plots and state-of-charge of rechargeable Ni–MH and Ni–Cd alkaline batteries. Although *iso*-frequency imaginary and real components exhibit significant dependency on SoC, especially at 0.1 Hz, no clear-cut dependency on SoC was found because the variations are not regular to enable unique SoC deduction. The same conclusion is drawn for the ohmic resistance, R_Ω, measured in the high frequency domain.

On the contrary, the series resonance frequency $f_\pm$ exhibits a reproducible monotonous dependency on SoC, either when measured after intermittent charges or discharges. Therefore, it can be concluded that this parameter, which is fast and easy to measure, is effective for routine monitoring the state-of-charge of the tested batteries. This observation must be extended over a wider range of batteries; it does provide strong grounds to pursue ac impedance techniques as probes of state-of-charge of vented and sealed in-service batteries.

Fig. 9. Evolution of the ohmic resistance with SoC for Ni–MH battery.

References

[1] R.T. Barton, P.J. Mitchell, J. Power Sources 27 (1989) 287.

[2] Ph. Blanchard, J. Appl. Electrochem. 22 (1992) 1121.

[3] V.V. Viswanathan, A.J. Salkind, J.J. Kelley, J.B. Ockerman, J. Appl. Electrochem. 25 (1995) 716.

[4] V.V. Viswanathan, A.J. Salkind, J.J. Kelley, J.B. Ockerman, J. Appl. Electrochem. 25 (1995) 729.

[5] N.A. Hampson, S.A.G.R. Karunathilaka, R. Leek, J. Appl. Electrochem. 10 (1980) 3.

[6] F. Huet, J. Power Sources 70 (1998) 59.

[7] S. Rodrigues, N. Munichandraiah, A.K. Shukla, J. Power Sources 87 (2000) 12.

[8] K. Bundy, M. Karlsson, G. Lindbergh, A. Lundqvist, J. Power Sources 72 (1998) 118.

[9] R. Haak, C. Ogden, D. Tench, J. Power Sources 12 (1984) 289.

[10] M. Hughes, R.T. Barton, S.A.G.R. Karunathilaka, N.A. Hampson, R. Leek, J. Appl. Electrochem. 15 (1985) 129.

[11] R. Heron, M.C. Fadden, J. Dunn, in: Proceedings of the Intellectual Conference, Vancouver, Canada, 1994, p. 270.

[12] E. Karden, S. Buller, R.W. De Doncker, J. Power Sources 85 (2000) 72.

[13] M.A. Reid, J. Power Sources 29 (1990) 467.

[14] M. Keddam, Z. Stoynov, H. Takenouti, J. Appl. Electrochem. 7 (1977) 539.

[15] X.Y. Xiong, H. Vander Poorten, M. Crappe, Electrochim. Acta 41 (1996) 1267.

[16] D. Linden, in: D. Linden (Ed.), Handbook of Batteries, Mc-Graw Hill, New York, 1995, pp. 33.1–33.29.

[17] B. Savova-Stoynov, Z.B. Stoynov, J. Appl. Electrochem. 17 (1987) 1150.

[18] W.L. Zhang, M.P.S. Kumar, S. Srinivasan, J. Electrochem. Soc. 142 (1995) 2935.

[19] X. Andrieu, P. Poignat, Power Sources 14 (1995) 43.